

## REMOTE SENSING OF ATMOSPHERE, HYDROSPHERE, AND UNDERLYING SURFACE

### Possibility of Clear Air Turbulence Localization with Lidar

V. A. Banakh<sup>a, \*</sup>, I. N. Smalikhov<sup>a, \*\*</sup>, and I. V. Zaloznaya<sup>a, \*\*\*</sup>

<sup>a</sup> V.E. Zuev Institute of Atmospheric Optics, Siberian Branch, Russian Academy of Sciences, Tomsk, 634055 Russia

\*e-mail: banakh@iao.ru

\*\*e-mail: smalikhov@iao.ru

\*\*\*e-mail: iya@iao.ru

Received June 27, 2022; revised August 1, 2022; accepted October 15, 2022

**Abstract**—The ranges of the parameters of wind and temperature (refractive) turbulence are estimated corresponding to the four-point scale of turbulence intensity at flight altitudes in the free atmosphere. It is shown that the estimates of both the variance of the radial velocity measured with a coherent lidar in the flight direction and of the structural constant of the refractive index from the lidar measurements of the intensity of refractive turbulence in the flight direction make it possible to judge the potential danger of bumpy flight of aircraft in clear-air turbulence zones ahead of the aircraft.

**Keywords:** clear air turbulence, wind lidar, turbulent energy dissipation rate, radial velocity variance, structural constant of turbulent fluctuations of the refractive index

**DOI:** 10.1134/S102485602303003X

Aircraft measurements [1] have shown turbulence to occur in the upper troposphere (at altitudes of 6–10 km) and lower stratosphere (up to ~25 km) with a relative frequency of up to 25% mainly in discontinuous (with characteristic horizontal sizes of individual parts of ~10 km) and continuous (with horizontal sizes of ~100 km) zones that drift with an average air flow. The vertical size of a turbulent zone is ~1 km. These zones are dangerous to aircraft under clear sky conditions. To reduce the risk of accidents, it is important to localize them in advance ahead of aircraft.

Clear-air turbulence (CAT) is usually assessed in terms of the degree of impact on the aircraft flight stability on a four-point scale: light ( $b_1$ ), moderate ( $b_2$ ), severe ( $b_3$ ), and extreme ( $b_4$ ). Based on the experimen-

tal data for the turbulence spectrum of the longitudinal wind velocity component in the free atmosphere

$$S_u(\kappa) = (2\pi)^{-1} \int_{-\infty}^{+\infty} dr B_u(r) \exp(-j\kappa r)$$

at  $\kappa = 2 \times 10^{-3} \text{ m}^{-1}$  [1] and with allowance for the possible spectrum definition  $S_u(\kappa) = 0.25\epsilon^{2/3} \kappa^{-5/3}$  when estimating the turbulent energy  $\int_{\kappa_1}^{\kappa_2} d\kappa S_u(\kappa)$  in the spectral range of aircraft-affecting inhomogeneities from  $\kappa_1 = 3 \times 10^{-4}$  to  $\kappa_2 = 3 \times 10^{-1} \text{ m}^{-1}$ , we have calculated the turbulence energy dissipation rates  $\epsilon$  in correspondence with this four-point scale (Table 1).

**Table 1.** Ranges of the parameters characterising the intensity of CAT

| Intensity of CAT, point | Turbulence energy dissipation rate $\epsilon$ , $\text{m}^2/\text{s}^3$ | Doppler spectrum width $\sigma_S$ , $\text{m/s}$ | Radial velocity variance $\sigma_r^2$ , $\text{m}^2/\text{s}^2$ | Structural constant of air refractive index fluctuations $C_n^2$ , $\text{m}^{-2/3}$ |
|-------------------------|---|--|---|--|
| $b_1$                   | $10^{-3} - 5 \times 10^{-3}$  | 0.97–1.65  | 0.9–2.7   | $3.5 \times 10^{-14} - 10^{-13}$   |
| $b_2$                   | $5 \times 10^{-3} - 1.5 \times 10^{-2}$                                 | 1.65–2.39  | 2.7–5.7   | $10^{-3} - 2.1 \times 10^{-13}$  |
| $b_3$                   | $(1.5 - 4.5) \times 10^{-2}$  | 2.39–3.45  | 5.7–11.8  | $(2.1 - 4.4) \times 10^{-13}$  |
| $b_4$                   | $\geq 4.5 \times 10^{-2}$   | $\geq 3.45$                                      | $\geq 11.8$   | $\geq 4.4 \times 10^{-13}$   |

Thus, measuring the turbulence kinetic energy dissipation rate in the flight direction, the location of CAT zones along the aircraft course can be detected in advance and the potential hazard can be estimated. Pulsed coherent Doppler lidars can be used for these purposes.

An important point in the lidar detection of CAT zones during a flight is the promptness of receiving necessary data. Assessment of the turbulence kinetic energy dissipation rate by the method of the azimuthal structure function [2] or from the spectra of turbulent fluctuations of the radial velocity [3] requires not only long-term measurements (about half an hour under ground conditions), but also a long time for iterative computation of the dissipation rate. In this work, we analyze a possibility of localizing CAT from other parameters of atmospheric turbulence, which can be remotely determined with lidars.

The most suitable technique for detection of CAT zones with coherent lidars is the estimation of the wind turbulence strength from broadening the Doppler power spectrum because of a random (due to wind turbulence) spread in the velocities of scattering particles in a volume sounded. The Doppler spectrum width (provided that the signal time window  $T_w$  significantly exceeds the sounding pulse duration  $\tau_p$ ) can be estimated by the simple formula [4]:

$$\sigma_s^2 = (\lambda/2)^2 / (8\pi^2 \sigma_p^2) + 0.45\varepsilon^{2/3} (T_w c/2)^{2/3}, \quad (1)$$

where  $\sigma_p = \tau_p / (2\sqrt{\ln 2})$ ;  $\lambda$  is the wavelength;  $c$  is the speed of light. The results of numerical simulation [4] for the lidar [5] with the parameters  $\lambda = 2.09 \mu\text{m}$ ,  $\tau_p = 400 \text{ ns}$ , and  $T_w = T_s M = 20.48 \mu\text{s}$ , where  $T_s = 20 \text{ ns}$  is the sampling time of a complex signal;  $M = 1024$  is the number of samples, confirm a possibility of estimating the intensity of turbulence ahead of the aircraft from the width of the Doppler spectrum of such lidars.

Table 1 presents the Doppler spectrum width calculated for these parameters and corresponding to different levels of turbulence  $\varepsilon$ . In the absence of turbulence ( $\varepsilon = 0$ ), the Doppler spectrum width is determined by the sounding pulse duration ( $\sigma_s \sim \lambda/\sigma_p$ ),  $\sigma_s \approx 0.49 \text{ m/s}$ , which is an order of magnitude larger than the spectral channel width in units of speed  $\Delta V = \lambda/(2T_w) \approx 0.05 \text{ m/s}$ . The spectrum broadens when turbulence appears. According to the table data, the spectrum width  $\sigma_s > 0.97 \text{ m/s}$  already under weak turbulence ( $b_1$ ) for the parameters  $\sigma_p$  and  $T_w$  selected. As the turbulence becomes stronger, the spectrum widens to  $3.45 \text{ m/s}$  and more, which can serve an indicator of CAT zones (this spectrum width ( $3.45 \text{ m/s}$ ) is approximately seven times larger than the above estimate of the instrumental spectrum broadening ( $0.49 \text{ m/s}$ )).

However, this is not completely true for coherent all-fiber lidar systems with shorter sounding pulses and signal sampling time (for example,  $\tau_p = 170 \text{ ns}$  and

$T_s = 20 \text{ ns}$  for a StreamLine all-fiber lidar (Halo Photonics, UK)). For this lidar with  $\lambda = 1.5 \mu\text{m}$ , the instrumental spectrum broadening  $\sigma_s = 1.5 \text{ m/s}$  if  $T_w = 120 \text{ ns}$  and  $0.83 \text{ m/s}$  if  $T_w \gg \tau_p$ . At  $T_w = T_s M = 20.48 \mu\text{s}$ , the turbulent broadening of the spectrum is also  $3.45 \text{ m/s}$  at  $\varepsilon = 4.5 \times 10^{-2} \text{ m}^2/\text{s}^3$ , which corresponds to the  $b_4$  level.

Thus, while the turbulent spectrum broadening at the storm level is seven times greater than the instrumental broadening for the lidar [5], the broadening at the same level of turbulence exceeds the instrumental one by  $3.45/0.83 \approx 4$  times as a maximum in all-fiber lidars. When narrowing the time window  $T_w$ , the instrumental spectrum broadening finally prevails over the turbulent one at any level of turbulence, which can be an obstacle to reliable detection of CAT zones.

This problem can be solved with the use of short-pulse all-fiber Doppler lidars based not only on the estimation of the turbulent broadening of the Doppler spectra, but also on other characteristics of the data measured, for example, on the variance of the radial velocity. In contrast to the dissipation rate, the estimation of the radial velocity variance from the initial lidar data does not require much time and can be carried out in real time with the current update according to the next estimate of the radial velocity from a distance specified. To estimate the radial velocity variance in the atmospheric boundary layer with an acceptable error, half-hour measurement series are required, like for estimation of the turbulence kinetic energy dissipation rate. However, during lidar measurements from aircraft, averaging due to the aircraft motion occurs along with averaging due to the drift of turbulent air inhomogeneities with a mean wind speed (which is usually much higher at aircraft flight altitudes than near the surface). At an aircraft speed of  $800\text{--}900 \text{ km/h}$ , an additional “drift” of turbulent inhomogeneities occurs at a speed of  $220\text{--}250 \text{ m/s}$ , which significantly (by about 40 times) reduces the averaging time as compared to ground-based measurements, down to  $45 \text{ s}$  on average. If we take into account that the mean wind speed at such altitudes is several tens of meters per second and is several times higher than the wind speed in the atmospheric boundary layer, then less than  $20 \text{ s}$  is actually required for the accurate estimate of the radial velocity variance. For this time, the aircraft flies no more than  $5 \text{ km}$ , and a pilot has time to make a decision if an echo signal is received from a distance of  $10\text{--}15 \text{ km}$ .

The equation for integral longitudinal scale of wind velocity turbulence,

$$L_V = \frac{1}{\varepsilon} \left( \frac{\sigma_r^2}{C_2} \right)^{3/2}, \quad (2)$$

where  $C_2 \approx 1.2717$ . Derived in [6] under the assumption of the applicability of the Karman turbulence

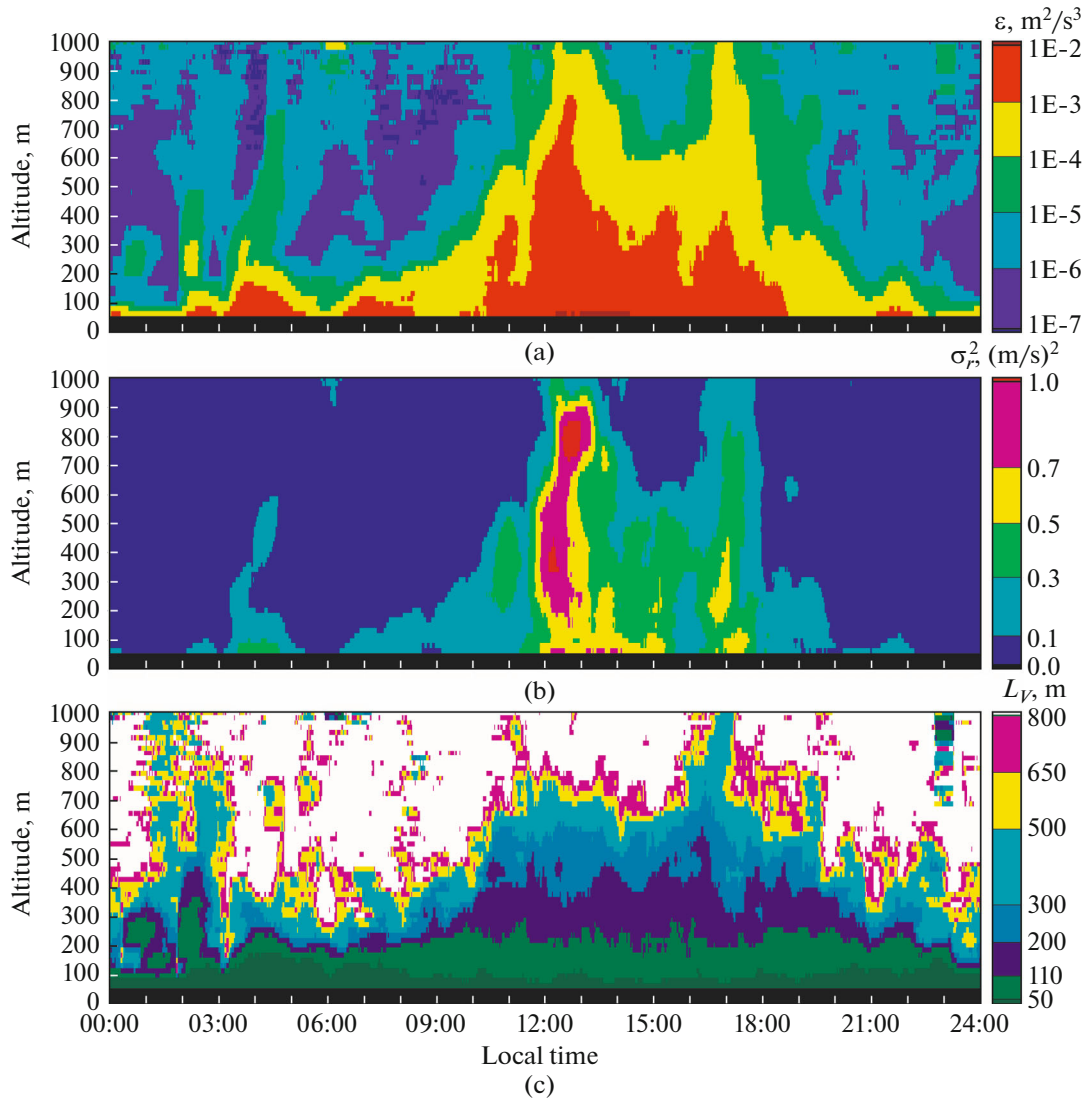


**Fig. 1.** Altitude and time distributions of the (a) turbulence kinetic energy dissipation rate, (b) radial velocity variance, and (c) integral longitudinal turbulence scale derived from StreamLine lidar measurements at BEO IAO SB RAS on July 21, 2019.

model, allows one to connect  $\varepsilon$  with the variance of the lidar-measured radial velocity  $\sigma_r^2$ :

$$\sigma_r^2 = C_2(\varepsilon L_V)^{2/3}. \quad (3)$$

To compare  $\varepsilon$  and  $\sigma_r^2$  (3), we used StreamLine coherent wind lidar measurements in the atmospheric boundary layer. The measurements were performed at the Basic Experimental Observatory (BEO) of the V.E. Zuev Institute of Atmospheric Optics, Siberian Branch, Russian Academy of Sciences (IAO SB RAS), on July 21, 2019, when a strong smog from wildfires was observed in Tomsk and the lidar signal-to-noise ratio (SNR) was quite high (no less than  $-15$  dB, mostly higher than  $-10$  dB, and sometimes 0 dB) within the kilometer-thick surface air layer. That ensured high accuracy of estimates of  $\varepsilon$  from the lidar data. In most cases, the

relative error in the dissipation rate  $E_\varepsilon$  calculated by the algorithm [7] did not exceed 30% provided that  $\varepsilon \geq 10^{-5} \text{ m}^2/\text{s}^3$ . Therefore, the estimates of  $\varepsilon$  and  $\sigma_r^2$  were compared for  $\varepsilon \geq 10^{-5} \text{ m}^2/\text{s}^3$ .

The lidar measurements were carried out with conical scanning by a sounding beam around the vertical axis at the elevation angle  $\varphi = 35.3^\circ$ . A detailed description of the experiment is given in [8]. Figure 1 shows two-dimensional distributions  $\varepsilon(h_k, t_n)$ ,  $\sigma_r^2(h_k, t_n)$ , and  $L_V(h_k, t_n)$  over altitude  $h_k = h_0 + k\Delta h$  and time  $t_n = n\Delta t$ , where  $h_0 = 58 \text{ m}$ ;  $k = 0, 1, 2, 3, \dots$ ;  $\Delta h = \Delta R \sin \varphi = 17.3357 \text{ m}$ ,  $\Delta R = 30 \text{ m}$  is the range step;  $n = 0, 1, 2, 3, \dots$ ;  $\Delta t = 0.035346 \text{ h}$  (2 min 7 s), calculated from the lidar measurements of the radial velocity. White color means that the  $L_V$  estimates exceed 800 m and are

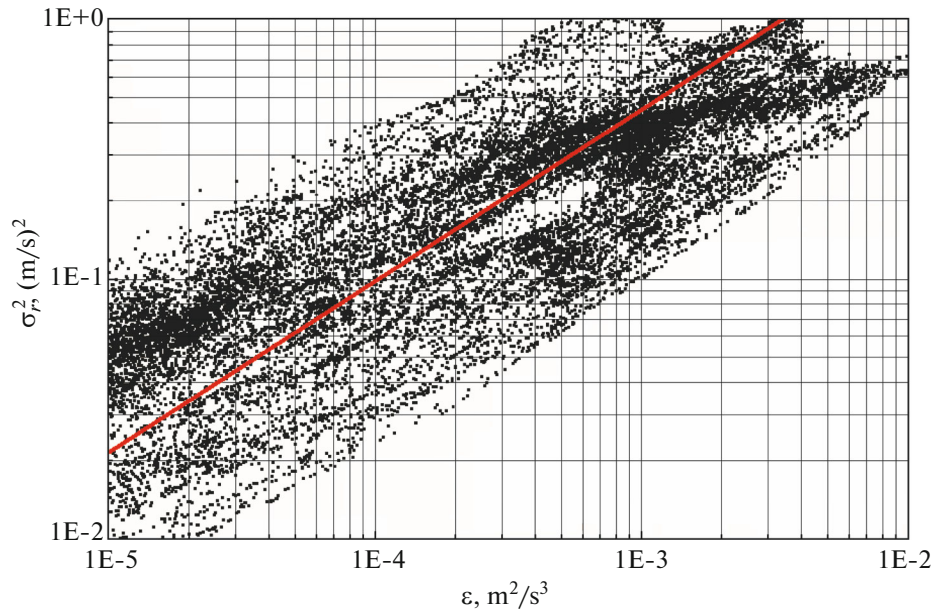


**Fig. 2.** Lidar estimates of the dissipation rate and the radial velocity variance taken from Figs. 1a and 1b (points); result of fitting  $\sigma_r^2(\varepsilon)$  (3) ( $L_V = 200$  m) to the estimates (red line).

incorrect for these altitudes. A similar altitude–time distribution of the relative error in the lidar estimate of the dissipation rate  $E_\varepsilon(h_k, t_n)$  was also calculated.

The lidar estimates of  $\varepsilon$  and  $\sigma_r^2$  taken from Figs. 1a and 1b, respectively, are compared in Fig. 2. According to the theoretical model used (Eq. (3)), the dependence of the variance of the radial velocity on the dissipation rate obeys the power law with the exponent “2/3” ( $\sigma_r^2 \sim \varepsilon^{2/3}$ ). The result of the least-squares fit of the dependence  $\sigma_r^2(\varepsilon)$  calculated by Eq. (3) at the fixed value  $L_V = 200$  m is shown by the red line in Fig. 2.

Thus, the integral scale in the atmospheric boundary layer, where  $\varepsilon \geq 10^{-5}$  m<sup>2</sup>/s<sup>3</sup> (green, yellow, and brown areas in Fig. 1a), averages approximately 200 m. As can be seen in Fig. 1c, the integral scale significantly varies with  $h_k$  and  $t_n$ , especially with altitude (mainly  $L_V$  increases with altitude) within these regions. This explains the quite wide scatter of points around the red line (at a fixed  $\varepsilon$ ) in Fig. 2.

The analysis of Figs. 1 and 2 shows that up to 90% of the  $\sigma_r^2$  estimates at fixed  $\varepsilon$  have been derived at the integral scale values from 50 to 800 m.

The experimental confirmation of dependence (3) by the data in Fig. 2 allows us to use it for estimating the radial velocity variance ranges corresponding to the four-point scale of aircraft flight stability. Data [1] imply that the integral turbulence scale  $L_V$  varies from 100 m to 1.9 km and is 630 m on average at altitudes of 10–12 km. The  $\sigma_r^2$  ranges calculated for  $L_V = 630$  m are

given in the 4th row of Table 1. The values of the radial velocity variance evidently significantly differ for different levels of the aircraft “bumpiness”; therefore, the variance can be used as an indicator of a CAT.

Attempts to design lidars for measuring the optical turbulence strength are known [9–11]. Experimental prototypes of the lidars exist today [10, 11]. Although their capability of receiving real-time information about CAT is not evident, the question is quite in order about the range of variations in the structural constant of turbulent fluctuations of the air refractive index  $C_n^2$ , which characterizes the intensity of a refractive turbulence, corresponding to the range of  $\varepsilon$  values in Table 1. The relationship [12]:

$$C_T^2 = a^2 \varepsilon^{-1/3} K_T (\partial T / \partial z)^2, \quad (4)$$

with connects the structural constant of the temperature and the turbulence kinetic energy dissipation rate, allows to do that. Here,  $a$  is the constant on the order of unity;  $K_T$  is the turbulent heat diffusivity coefficient;  $\partial T / \partial z$  is the vertical gradient of the potential temperature. Hence, lidars which make possible estimation of  $C_n^2$  can be used for detection of CAT zones ( $C_T^2$  and  $C_n^2$  are connected by the well known relationship from [12]).

At air traffic altitudes of 10–11 km, the thermal stratification of the atmosphere is stable. Based on the two-parameter theory of turbulent closure by Zilitinkevich [13], we can write

$$C_T^2 = A \varepsilon^{2/3}, \quad (5)$$

where  $A = 1.85 \text{ K}^2 \text{ s}^2/\text{m}^2$  is the dimensional constant, under the assumption that the mean absolute temperature is equal to 220 K and the potential temperature gradient  $\partial T/\partial z = 0.0033 \text{ K/m}$  at altitudes from 10 to 11 km according to the standard model of the atmosphere.

The  $C_n^2$  values calculated by Eq. (5) with the use of the relationship between  $C_T^2$  and  $C_n^2$  [12] are given in Table 1 for the ranges of  $\varepsilon$  corresponding to the four-point scale of the intensity of CAT. One can see that  $C_n^2$  changes by more than an order of magnitude, from  $3.5 \times 10^{-14}$  to  $4.4 \times 10^{-13} \text{ m}^{-2/3}$ , which makes it possible to use the structural constant of turbulent fluctuations of the air refractive index for CAT localization.

Thus, the analysis of experimental data and theoretical calculations has shown that the potential danger of aircraft bumpy flight in CAT zones ahead of the aircraft can be estimated from both the variance of the radial velocity measured with a pulsed coherent wind lidar and the structural constant of the air refractive index derived from the lidar measurements of the intensity of refractive turbulence in the flight direction.

#### FUNDING

The theoretical and experimental studies of a possibility of lidar localization of CAT zones were supported by the Russian Science Foundation (project 19-17-00170-P). The development of the measurement methodology and support of the infrastructure of the Basic Experimental Observatory of the IAO SB RAS were supported by the Ministry of Science and Higher Education of the Russian Federation (V.E. Zuev Institute of Atmospheric Optics, Siberian Branch, Russian Academy of Sciences).

#### CONFLICT OF INTEREST

The authors declare that they have no conflicts of interest.

#### OPEN ACCESS

This article is licensed under a Creative Commons Attribution 4.0 International License, which permits use, sharing, adaptation, distribution and reproduction in any medium or format, as long as you give appropriate credit to the original author(s) and the source, provide a link to the Creative Commons license, and indicate if changes were made. The images or other third party material in this article are included in the article's Creative Commons license, unless indicated otherwise in a credit line to the material. If material is not included in the article's Creative Commons license and your intended use is not permitted by statutory regulation or exceeds the permitted use, you will need to obtain permission directly from the copyright holder. To view a copy of this license, visit <http://creativecommons.org/licenses/by/4.0/>.

#### REFERENCES

1. N. K. Vinnichenko, N. Z. Pinus, S. M. Shmeter, and G. N. Shur, *Turbulence in the Free Atmosphere* (Springer Science+Business Media New York, 1980).
2. I. N. Smalikho and V. A. Banakh, "Measurements of wind turbulence parameters by a conically scanning coherent Doppler lidar in the atmospheric boundary layer," *Atmos. Meas. Tech.* **10** (11), 4191–4208 (2017).
3. V. A. Banakh, I. N. Smalikho, A. V. Falits, and A. M. Sherstobitov, "Estimating the parameters of wind turbulence from spectra of radial velocity measured by a pulsed Doppler lidar," *Remote Sens.* **13**, 2071 (2021).
4. V. A. Banakh, Ch. Werner, and I. N. Smalikho, "Remote sensing of clear sky turbulence using Doppler lidar. Numerical simulation," *Atmos. Ocean. Opt.* **14** (10), 856–863 (2001).
5. S. W. Henderson, Ch. P. Hale, J. R. Magee, M. J. Kavaya, and A. V. Huffaker, "Eye-safe coherent laser radar system at 2  $\mu\text{m}$  using Tm,Ho:YAG Lasers," *Opt. Lett.* **16**, 773–775 (1991).
6. I. N. Smalikho and V. A. Banakh, "Accuracy of estimation of the turbulent energy dissipation rate from wind measurements with a conically scanning pulsed coherent Doppler Lidar. Part I. Algorithm of data processing," *Atmos. Ocean. Opt.* **26** (5), 404–410 (2013).
7. V. A. Banakh, I. N. Smalikho, and V. A. Falits, "Estimation of the turbulence energy dissipation rate in the atmospheric boundary layer from measurements of the radial wind velocity by micropulse coherent Doppler lidar," *Opt. Express* **25** (19), 22679–22692 (2017).
8. V. A. Banakh, I. N. Smalikho, and A. V. Falits, "Determination of the height of the turbulent mixing air layer based on estimation of the parameters of wind turbulence from lidar data," *Opt. Atmos. Okeana* **34** (3), 169–184 (2021).  
<https://doi.org/10.15372/AOO20210303>
9. A. S. Gurvich, "Lidar sounding of turbulence based on the backscatter enhancement effect," *Izv., Atmos. Ocean. Phys.* **48** (6), 585–594 (2012).
10. P. Vrancken, M. Wirth, G. Ehret, H. Barny, P. Rondeau, and H. Veerman, "Airborne forward-pointing UV Rayleigh lidar for remote clear air turbulence detection: System design and performance," *Appl. Opt.* **55** (32), 9314–9328 (2016).
11. A. Hauchecorne, Ch. Cot, F. Dalaudier, J. Porteneuve, T. Gaudo, R. Wilson, C. Cenac, Ch. Laqui, P. Keckhut, J.-M. Perrin, A. Dolfi, N. Cezard, L. Lombard, and C. Besson, "Tentative detection of clear-air turbulence using a ground-based Rayleigh lidar," *Appl. Opt.* **55** (13), 3420–3428 (2016).
12. V. I. Tatarskii, *Wave Propagation in a Turbulent Atmosphere* (Dover Publications, Inc., New York, 2017).
13. S. S. Zilitinkevich, *Atmospheric Turbulence and Planetary Boundary Layer* (Fizmatlit, Moscow, 2013) [in Russian].

Translated by O. Ponomareva